

1 **Brief communication**

2 **Nonlinear sensitivity of glacier-mass balance to climate attested by**
3 **temperature-index models**

4 *Christian Vincent and Emmanuel Thibert*

5
6 *Université Grenoble Alpes, CNRS, IRD, Grenoble-INP, INRAE, Institut des Géosciences de*
7 *l'Environnement (IGE, UMR 5001), F-38000 Grenoble, France.*

8
9 Correspondence : *Christian Vincent* (christian.vincent@univ-grenoble-alpes.fr) and *Emmanuel Thibert*
10 (emmanuel.thibert@inrae.fr)

11

12 **Abstract**

13 Temperature-index models have been widely used for glacier-mass projections spanning the 21st
14 century. The ability of temperature-index models to capture nonlinear responses of glacier surface-mass
15 balance (SMB) to high deviations in air temperature and solid precipitation has recently been ~~questioned~~
16 ~~discussed in the context of~~by mass-balance simulations employing advanced machine-learning
17 techniques. Here, we performed numerical experiments with a classic ~~and simple~~ temperature-index
18 model and confirmed that such models are capable of detecting nonlinear responses of glacier SMB to
19 temperature and precipitation changes. Nonlinearities derive from the change of the degree-day factor
20 over the ablation season and from the lengthening of the ablation season.

21

22 **Introduction**

23 Glacier SMB projections in response to climate change up to the end of the 21st century can be analysed
24 via physical approaches using energy-balance calculations and empirical approaches linking simple
25 meteorological variables to SMB such as temperature-index models. Most glacier-mass projections in
26 response to climate change in large-scale studies spanning the 21st century have been based on

27 temperature-index models (Huss and Hock, 2015; Fox-Kemper *et al.*, 2021), given the lack of available
28 or reliable information on detailed future meteorological variables (Réveillet *et al.*, 2018). The deep
29 artificial neural network (ANN) approach is a promising new empirical approach to simulate SMB in
30 the future (Bolibar *et al.*, 2020). A neural network is a collection of interconnected simple processing
31 elements called neurons. These processing elements are assigned coefficients or weights, which
32 constitute the neural-network structure. Each weight is generated by the training process for the ANN
33 (Agatonovic-Kustrin and Beresford, 2000).

34 Recently, Bolibar *et al.* (2022) analysed the sensitivity of glacier SMB to future climate change using a
35 deep ANN. They write that, ~~unlike linear statistical and temperature index models,~~ their deep-learning
36 approach captures nonlinear responses of glacier SMB to high deviations in air temperature and solid
37 precipitation, improving the representation of extreme SMBs. Bolibar *et al.* (2022) argue that
38 temperature-index models, widely used to simulate the large-scale evolution of glaciers, ~~provide only~~
39 ~~linear relationships between positive degree days (PDDs), solid precipitation and SMB. can be suitable~~
40 ~~for steep mountain glaciers, but may be less suitable for some scenarios and flatter glaciers and ice caps~~
41 ~~due to linear sensitivities in such mass balance models. Here, we performed numerical experiments with~~
42 ~~a classic and simple temperature index model and the results demonstrated nonlinear responses of~~
43 ~~glacier SMB to temperature and precipitation changes. In this paper we perform numerical experiments~~
44 ~~with a classic and simple temperature-index model. Our unique purpose is to demonstrate that~~
45 ~~temperature-index models are able to capture nonlinear responses of glacier mass balance (MB) to high~~
46 ~~deviations in air temperature and solid precipitation.~~

Mis en forme : Police :(Par défaut) Times New Roman

Mis en forme : Police :(Par défaut) Times New Roman

47

48 **Data**

49 For our numerical experiments, we selected two very different glaciers in the French Alps. The first, the
50 Argentière Glacier, is located in the Mont-Blanc range (45°55' N, 6°57'E). Its surface area was
51 approximately 10.9 km² in 2018. The glacier extends from an altitude of approximately 3 400 m a.s.l. at
52 the upper bergschrund down to 1 600 m a.s.l. at the snout. It faces north-west, except for a large part of
53 the accumulation area (south-west facing tributaries). The second, the Sarennes Glacier, is a small south-
54 facing glacier (0.51 km²) with a limited altitude range between 2 820 m and 3 160 m (mean values over

55 the period used for the present study), located in the Grande Rousses range (45°07'N; 6°07'E). The field
56 SMB observations of the Argentière and Sarennes glaciers come from the French glacier monitoring
57 program GLACIOCLIM (Les GLACIers, un Observatoire du CLIMat; <https://glacioclim.osug.fr/>).
58 Annual SMBs were monitored in the ablation area of the Argentière Glacier between 1975 and 1993,
59 using 20 to 30 ablation stakes. Since 1993, systematic winter and summer mass-balance measurements
60 (May and September respectively) have been carried out over the entire surface of the glacier.
61 Approximately 40 sites were selected at various elevations representative of the whole surface.
62 Moreover, geodetic mass balances have been calculated using Digital Elevation Models on the basis of
63 an old map from 1905 and photogrammetric measurements carried out in 1949, 1980, 1993, 1998, 2003,
64 2008 and 2019 (Vincent *et al.*, 2009). Since 1949, systematic winter and summer mass-balance
65 measurements have been carried out on the Sarennes glacier, from which annual balances are calculated
66 (Thibert *et al.*, 2013).

67 We used the atmospheric temperature and precipitation data from the SAFRAN (Système d'Analyse
68 Fournissant des Renseignements Adaptés à la Nivologie, Analysis system for the provision of
69 information for snow research) reanalysis process that are available from 1958 to date (Durand *et al.*,
70 2009; Verfaillie *et al.*, 2018). SAFRAN disaggregates large-scale meteorological analyses and
71 observations in the French Alps. The analyses provide hourly meteorological data as a function of seven
72 slope exposures (N, S, E, W, SE, SW and flat) and altitude (at 300 m intervals up to 3 600 m a.s.l), and
73 that differ for each mountain range (e.g. Mont Blanc, Vanoise and Grandes Rousses ranges).

74

75 **Method**

76 We ran numerical experiments with a classic simple temperature-index model (Hock, 1999; Reveillet *et*
77 *al.*, 2017) and using SAFRAN reanalysis data (Durand *et al.*, 2009; Verfaillie *et al.*, 2018). These
78 numerical experiments were run on the two very different French glaciers, Argentière and Sarennes,
79 observed over several decades (Thibert *et al.*, 2013; Vincent *et al.*, 2009). The SMB model was run for
80 each day using the equation:

81 $SMB = DDF_{snow/ice} \cdot T + k \cdot P,$

82 Where:

- 83 - T is the difference between the mean daily air temperature and the melting point,
- 84 - $DDF_{\text{snow/ice}}$ is the degree-day factor for snow and ice and $DDF=0$ if $T<0^{\circ}\text{C}$,
- 85 - P is the precipitation (m w.e.),
- 86 - k is a ratio between snow accumulation and precipitation and $k=0$ if $T>0^{\circ}\text{C}$.

87 The degree-day factors for snow and ice were 0.0035 and 0.0055 m w.e. $\text{K}^{-1}\text{d}^{-1}$ for the Argentière glacier
88 (Reveillet *et al.*, 2017) and 0.0041 and 0.0068 m w.e. $\text{K}^{-1}\text{d}^{-1}$ for the Sarennes glacier (Thibert *et al.*,
89 2013). The point-mass balances were calculated for each elevation, for the Argentière and Sarennes
90 glaciers. In addition, we calculated the glacier-wide mass balance of the Argentière glacier using the
91 point-mass balances for the elevation range and the geodetic mass balances (Vincent *et al.*, 2009).
92 Parameter k depends on the site elevation in accounting for the precipitation gradient and is determined
93 from the winter-balance measurements and precipitation data.

94 Other enhanced temperature-index models including potential direct solar radiation could be used for
95 our study, but here the purpose is to show that responses in SMB are not linear to temperature or
96 precipitation changes even using a simple degree-day model.

97

98 **Results**

99 The reconstruction of the glacier-wide MBs of these glaciers from our simple temperature-index model
100 shows good agreement with data (Fig. 1). Using these reconstructed MBs, we calculated the SMB
101 sensitivities to temperature and winter precipitation at 2 750 metres and 3 100 metres on the Argentière
102 and Sarennes glaciers respectively (Fig. 2). These altitudes were selected because they correspond to
103 the approximate center of the glaciers. For each day of each series, we calculated an annual SMB
104 anomaly by adding a temperature anomaly or a precipitation anomaly. The anomaly was generated as a
105 shift (increment/decrement) of the mean of the distribution of the original data in temperatures and
106 winter balances. The distribution around the means was unchanged (same year-to-year variability as
107 found in the original data).

108 We report the results in Figure 2 to mirror Figure 3 of Bolibar *et al.* (2022) and make the comparison
109 easier. We also ran these numerical experiments at different altitudes and over the entire glacier surface
110 of the Argentière glacier (Fig. 3).

111 From our experiments, we found first that the response of SMB to temperature, using a temperature-
112 index model, is not linear, ~~contrary to the conclusions of Bolibar *et al.* (2022) relative to temperature-~~
113 ~~index models.~~ As expected, the sensitivity of annual SMB (i.e. the slope of the green curves in the graphs
114 of Figure 2) increases with the PDD anomaly. To explain the physical processes involved in
115 nonlinearity, we again used our PDD model, but using synthetic data for atmospheric temperature
116 changes over a year (Fig. 4a). The reference scenario (unforced temperature and winter-balance
117 reference conditions) of synthetic data is typical for a location in the upper ablation area of an Alpine
118 glacier (cumulative PDD of 800 degree.days from early May to early October; 1 700 mm of winter
119 balance). We use increments of $\pm 1\text{K}$ (-5K ; $+5\text{K}$) to analyse the response of SMB. PDD factors for snow
120 and ice come from Thibert *et al.* (2013). As shown in Figure 4, the nonlinearity with respect to
121 temperature forcing (the spread between SMB plots in Fig.4c) comes from (i) the lengthening of the
122 ablation season (Fig.4a) and (ii) the earlier disappearance of the winter snow cover which increases the
123 ablation rate due to the change in the degree-day factor from snow to ice (Fig. 4b).

124 Concerning the winter balance, runs of our PDD model on synthetic data under different conditions of
125 winter balance (Fig. 5) used a reference scenario of 1 700 mm of winter balance changed by increments
126 of ± 300 mm in precipitation. We found a nonlinear response of SMBs to winter precipitation with our
127 PDD model ~~and this is also inconsistent with the conclusions of Bolibar *et al.* (2022) relative to the~~
128 ~~sensitivity of temperature index models.~~ For instance, with winter accumulation decreased by -
129 1500 mm, ice ablation starts very early (by the end of May) and the annual MB is $-5.55 \text{ m w.e. a}^{-1}$ in
130 October. With winter accumulation increased by +1500 mm, ice ablation starts in mid-September and
131 the annual MB is $-0.21 \text{ m w.e. a}^{-1}$ in October. This asymmetry clearly shows that the response to winter
132 accumulation is not linear. Results show that the increase in sensitivity can be physically explained by
133 the earlier disappearance of the winter snow cover. The earlier and abrupt increase in the ablation rate
134 under lower conditions of winter balance (Fig.5a) results in nonlinearity attested by the spread between
135 SMB plots in Figure 5b. ~~Surprisingly, w~~We detect sensitivity to winter accumulation, contrary to the

136 Bolibar *et al.* (2022) findings using their ANN (Fig. 2 and 3). Indeed, MB sensitivity increases with low
137 winter-accumulation anomalies using our model, but decreases in the deep-learning model of Bolibar *et*
138 *al.* (2022). Our results are consistent with direct in-situ observations (Six and Vincent, 2014) and also
139 consistent with the results reported by Reveillet *et al.* (2018) from observations and energy-balance
140 modelling. The opposite results obtained from the deep-learning model ~~are paradoxical and~~ may be due
141 to an issue in the calibration of the model.

142 Summing up, the ability of PDD models to provide nonlinear sensitivity to air temperature and solid
143 precipitation is due to the different ablation rates and the associated change in the degree-day factor that
144 can be involved depending on snow or ice conditions at the glacier surface. An additional nonlinearity
145 to temperature forcing is caused by changes in the ablation duration.

146 Another question arises in the Discussion section of Bolibar *et al.* (2022), concerning the comparison
147 between their results and those from other studies. ~~The authors claim that~~ According to this paper, all
148 glacier models in the Glacier Model Intercomparison Project (GlacierMIP) (Hock *et al.*, 2019) rely on
149 SMB models with linear relationships between PDDs, melt and precipitation. The authors argue that
150 these PDD models present behaviour very similar to the linear-build statistical LASSO model. ~~This is~~
151 ~~erroneous given that,~~ However most of the temperature-index models used in GlacierMIP include two
152 degree-day factors. Consequently, they cannot provide a linear response to climate forcing as shown
153 above. In the Bolibar *et al.* (2022) paper, the MB anomalies in response to climate forcing were obtained
154 using a linear LASSO SMB model, which is based on a regularized multi-linear regression, ~~although~~
155 ~~The choice of the LASSO model is even more surprising given that~~ the authors also used the
156 GloGEMflow model in their paper (see their Discussion section), which is a temperature-index model
157 widely used for glacier projections (Zekollari *et al.* 2019).

158

159 **Conclusions**

160 From ~~our~~ numerical experiments with a classic and simple temperature-index model, ~~we found nonlinear~~
161 ~~responses of glacier SMB to temperature and precipitation changes. These~~ our results question those of
162 Bolibar *et al.* (2022), who argue that temperature index models provide only linear relationships
163 ~~between positive degree days (PDDs), solid precipitation and SMB. highlight that temperature-index~~

164 models are able to capture nonlinear responses of glacier mass balance (MB) to high deviations in air
165 temperature and solid precipitation, unlike Bolibar *et al.* (2022) study.

Mis en forme : Police :Italique

166 ~~We tried to understand the cause of this discrepancy.~~ Bolibar *et al.* (2022) compared the response of
167 SMB to climate forcing (air temperature, winter and summer snow falls) using a deep-learning approach
168 and a LASSO model. From this comparison, they conclude that deep learning provides a nonlinear
169 response, contrary to the LASSO model. The conclusions of Bolibar *et al.* (2022) may be due to the use
170 of a linear LASSO SMB model instead of a temperature-index model. We would suggest testing the
171 capability of an ANN to capture nonlinearity by comparing its results with that of the GloGEM Positive
172 Degree-Day (PDD) model that they used in their paper.

173 Regarding specifically SMB changes due to solid precipitations, the deep-learning model used by
174 Bolibar *et al.* (2022) foresees decreasing sensitivity under low winter-accumulation conditions. We
175 point out that this result directly contradicts PDD model outcomes. We explain in physical terms why a
176 PDD model projects higher sensitivity to low winter accumulation, but do not yet understand why the
177 approach of Bolibar *et al.* (2022) does not.

178 Given that detailed meteorological variables are highly unpredictable in the future, most glacier-mass
179 projections in response to climate change in large-scale studies spanning the 21st century are still today
180 based on temperature-index models with simple temperature and precipitation variables. It follows that
181 the questions raised here relative to the nonlinear responses of surface SMB to meteorological variables
182 are crucial.

183

184 **Data availability**

185 This commentary does not include original data. All data referred to in the text have been published
186 elsewhere. Field data are accessible through the project website at <https://glacioclim.osug.fr>.

187 Results from the PDD simulations on synthetic data are accessible from the open data
188 repository: [10.5281/zenodo.7603415](https://doi.org/10.5281/zenodo.7603415).

189

190 **Author contributions**

191 ET and CV ran the numerical modelling calculations and produced the analysis. CV supervised the study
192 and wrote the paper. Both authors contributed to discussion of the results.

193

194 **Competing interests**

195 The authors declare that they have no conflicts of interest.

196

197 **Acknowledgements**

198 This study was funded by *Observatoire des Sciences de l'Univers de Grenoble (OSUG)* and *Institut des*
199 *Sciences de l'Univers (INSU-CNRS)* in the framework of the French GLACIOCLIM (*Les GLACIers,*
200 *un Observatoire du CLIMat*) program. We thank all those who conducted the field measurements. We
201 are grateful to Cary Bartsch for reviewing the English.

202

203 **References**

204

205 Agatonovic-Kustrin, S. and Beresford, R. : Basic concepts of artificial neural network (ANN) modeling
206 and its application in pharmaceutical research, *Journal of Pharmaceutical and Biomedical Analysis*, 22,
207 5, [https:// doi.org./ 10.1016/s0731-7085\(99\)00272-1](https://doi.org/10.1016/s0731-7085(99)00272-1),2000.

208

209 Bolibar, J., Rabatel, A., Gouttevin, I., Galiez, C., Condom, T., and Sauquet, E.: Deep learning applied
210 to glacier evolution modelling, *The Cryosphere*, 14, 565–584, <https://doi.org/10.5194/tc-14-565-2020>,
211 2020.

212

213 Bolibar, J., Rabatel, A., Gouttevin, I., Zekollari, H. and Galiez, C.: Nonlinear sensitivity of glacier mass
214 balance to future climate change unveiled by deep learning, *Nature Communications* 13, 409,
215 <https://doi.org/10.1038/s41467-022-28033-0>, 2022.

216

217 Durand, Y., Laternser, M., Giraud, G., Etchevers, P., Lesaffre, B. and Mérindol, L.: Reanalysis of 44 yr
218 of climate in the French Alps (1958–2002): Methodology, model validation, climatology, and trends for
219 air temperature and precipitation, *J. Appl. Meteorol. Clim.*, 48, 429–449,
220 <https://doi.org/10.1175/2008JAMC1808.1>, 2009.

221
222 Fox-Kemper, B., et al. Ocean, Cryosphere and Sea Level Change. In *Climate Change 2021: The*
223 *Physical Science Basis. Contribution of Working Group I to the Sixth Assessment Report of the*
224 *Intergovernmental Panel on Climate Change [Masson-Delmotte, V., P. Zhai, A. Pirani, S.L. Connors,*
225 *C. Péan, S. Berger, N. Caud, Y. Chen, L. Goldfarb, M.I. Gomis, M. Huang, K. Leitzell, E. Lonnoy,*
226 *J.B.R. Matthews, T.K. Maycock, T. Waterfield, O. Yelekçi, R. Yu, and B. Zhou (eds.)]. Cambridge*
227 *University Press, Cambridge, United Kingdom and New York, NY, USA, pp. 1211–1362,*
228 <https://doi:10.1017/9781009157896.011>, 2021.

229
230 Hock, R.: Temperature index melt modelling in mountain areas, *Journal of Hydrology*, 282, 1–4, 104–
231 115, [https://doi.org/10.1016/S0022-1694\(03\)00257-9](https://doi.org/10.1016/S0022-1694(03)00257-9), 2003.

232
233 Hock, R. et al.: GlacierMIP – A model intercomparison of global-scale glacier mass-balance models
234 and projections, *Journal of Glaciology*, 65 (251), 453-467, <https://doi:10.1017/jog.2019.22>, 2019.

235
236 Huss, M. and Hock, R.: New model for global glacier change and sea-level rise, *Front. Earth Sc.*, 3,
237 <https://doi:10.3389/feart.2015.00054>, 2015.

238
239 Marzeion, B., Cogley, J.G., Richter, K. and Parkes, D.: Attribution of global glacier mass loss to
240 anthropogenic and natural causes, *Science*, 345, 919-921, <https://doi:10.1126/science.1254702>, 2014.

241
242 Reveillet, M., Vincent, C., Six, D. and Rabatel, A.: Which empirical model is best suited to simulate
243 glacier mass balances ?, *J. Glaciol.*, 63, 39-54, <https://doi:10.1017/jog.2016.110>, 2017.

244

245 Réveillet, M., Six, D., Vincent, C., Rabatel, A., Dumont, M., Lafaysse, M., Morin, S., Vionnet, V., and
246 Litt, M.: Relative performance of empirical and physical models in assessing the seasonal and annual
247 glacier surface mass balance of Saint-Sorlin Glacier (French Alps), *The Cryosphere*, 12, 1367–1386,
248 <https://doi.org/10.5194/tc-12-1367-2018>, 2018.

249

250 Six, D. and Vincent, C.: Sensitivity of mass balance and equilibrium-line altitude to climate change in
251 the French Alps. *J. Glaciol.* 60, 867–878. doi:10.3189/2014JoG14J014, 2014.

252

253 Thibert, E., Eckert, N. and Vincent, C.: Climatic drivers of seasonal glacier mass balances: an analysis
254 of 6 decades at Glacier de Sarennes (French Alps), *The Cryosphere*, 7, 47–66, [https://doi.org/10.5194/tc-](https://doi.org/10.5194/tc-7-47-2013)
255 [7-47-2013](https://doi.org/10.5194/tc-7-47-2013), 2013.

256

257 Verfaillie, D., Lafaysse, M., Déqué, M., Eckert, N., Lejeune, Y. and Morin, S.: Multi-component
258 ensembles of future meteorological and natural snow conditions for 1500 m altitude in the Chartreuse
259 mountain range, Northern French Alps, *The Cryosphere*, 12, 1249–1271, [https://doi.org/10.5194/tc-12-](https://doi.org/10.5194/tc-12-1249-2018)
260 [1249-2018](https://doi.org/10.5194/tc-12-1249-2018), 2018.

261

262 Vincent, C., Soruco, A., Six, D. and Le Meur, E.: Glacier thickening and decay analysis from 50 years
263 of glaciological observations performed on Glacier d’Argentière, Mont Blanc area, France, *Ann.*
264 *Glaciol.*, 50 (50), 73-79, [https:// doi:10.31189/172756409787769500](https://doi.org/10.31189/172756409787769500), 2009.

265

266 Zekollari, H., Huss, M., and Farinotti, D.: Modelling the future evolution of glaciers in the European
267 Alps under the EURO-CORDEX RCM ensemble, *The Cryosphere*, 13, 1125–1146,
268 <https://doi.org/10.5194/tc-13-1125-2019>, 2019.

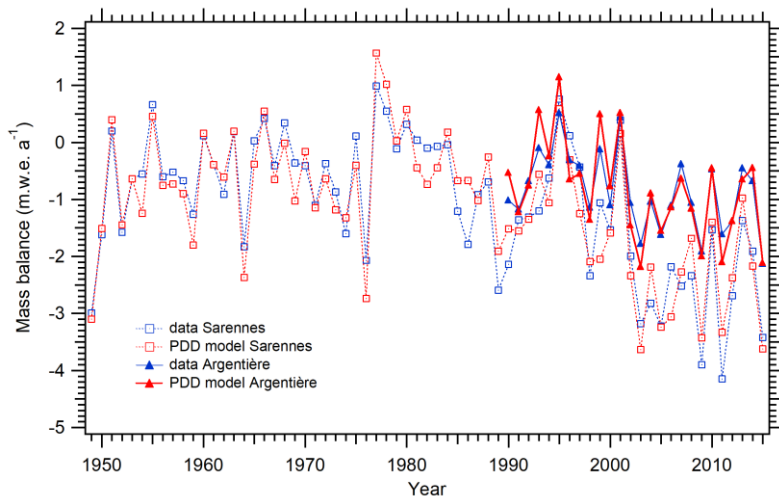
269

270

271

272

273



274

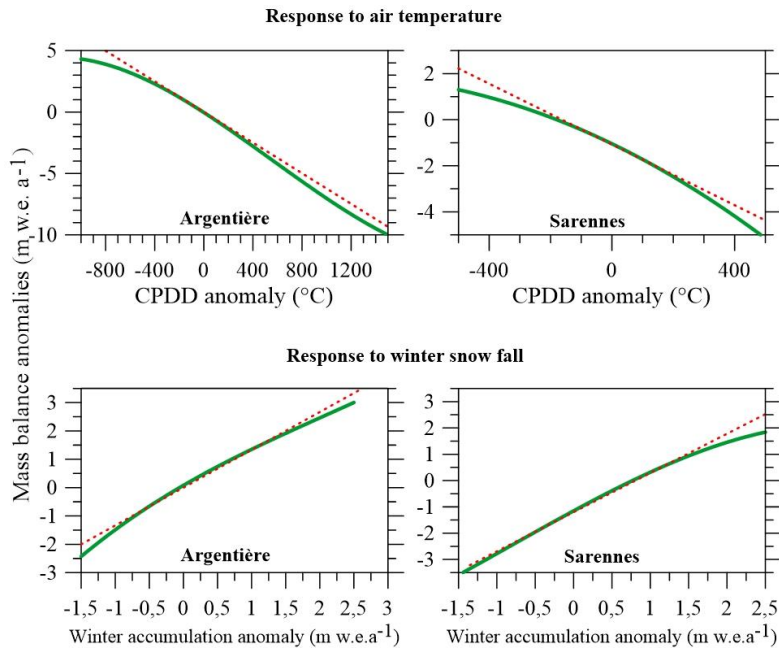
275 Figure 1. Glacier-wide mass balance of the Argentière glacier (1990-2015) and the Sarennes glacier

276 (1949-2015). Observations and simulations from the simple degree-day model used in our experiments.

277

278

279



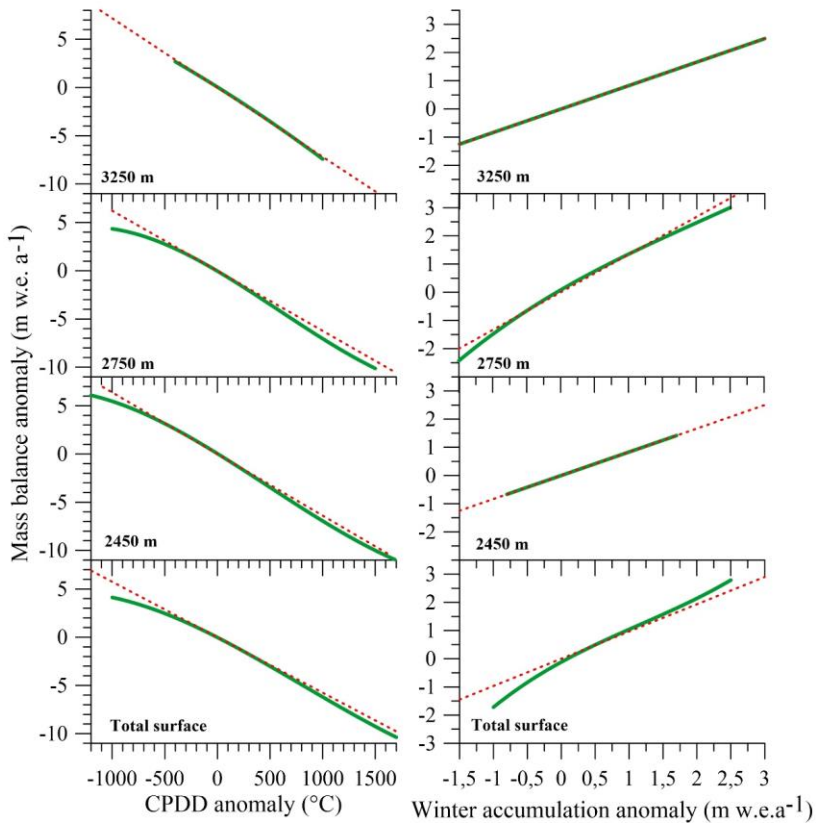
280

281 Figure 2. Response of mass balance to climate forcing using a temperature-index model (green line) at

282 2 750 m and 3 100 m on the Argentière (left panel) and Sarenes (right panel) glaciers, respectively.

283 The red dashed lines are the best linear fit. Note that in such graphs, the sensitivity of the mass balance

284 to temperature and winter accumulation changes is the slope of the curves.



286

287

288 Figure 3. Response of annual mass balance to air temperature (left panel) and to winter accumulation

289 (right panel) using a temperature-index model (green line) on the Argentiere glacier. The red dashed

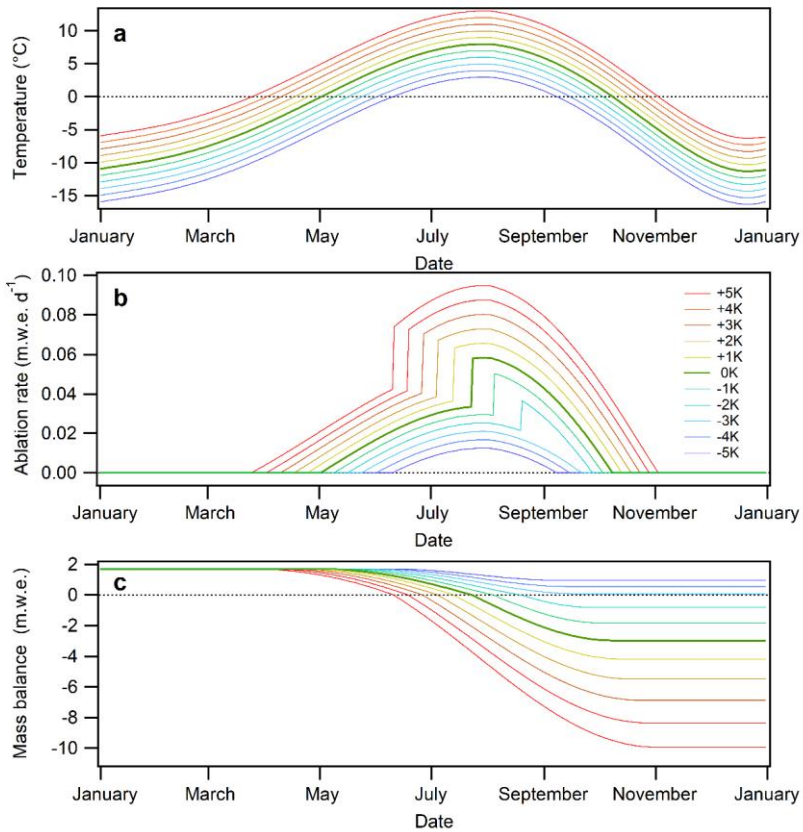
290 lines are the best fit forced through the origin.

291

292

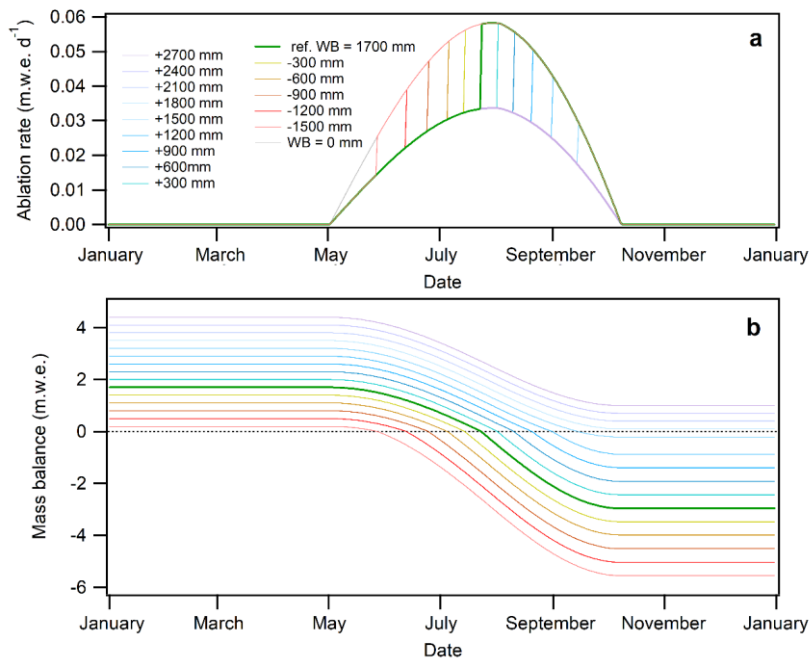
293

294



295
 296 Figure 4. Positive degree-day model running on synthetic data (response to air temperature). Evolution
 297 of air temperatures (a), ablation rates (b) and mass balance (c) over the year, according to different
 298 temperature scenarios, calculated at 2 800 m. Note the jump in ablation rates when ablation shifts from
 299 snow to ice. This occurs earlier with temperature forcing. Note also the lengthening of the ablation
 300 season with rise in temperature.

301
 302
 303



304
 305 Figure 5. Positive degree-day model running on synthetic data (response to winter balance). Change in
 306 ablation rates (a) and mass balance (b) over the year, according to different winter-balance scenarios
 307 calculated at 2 800 m. Note the jump in ablation rates when ablation shifts from snow to ice. This occurs
 308 earlier under lower winter-balance conditions. Note that the duration of the ablation season is unchanged
 309 under variable winter-balance conditions.

310
 311
 312
 313